Macromolecules

Article

pubs.acs.org/Macromolecules

Functional Poly(ε-caprolactone)s via Copolymerization of ε-Caprolactone and Pyridyl Disulfide-Containing Cyclic Carbonate: Controlled Synthesis and Facile Access to Reduction-Sensitive Biodegradable Graft Copolymer Micelles

Wei Chen,[†,‡] Yan Zou,[†] Junna Jia,[†] Fenghua Meng,[†] Ru Cheng,[†] Chao Deng,[†] Jan Feijen,[†,‡] and Zhiyuan Zhong*[,†]

[†]Biomedical Polymers Laboratory, and Jiangsu Key Laboratory of Advanced Functional Polymer Design and Application, Department of Polymer Science and Engineering, College of Chemistry, Chemical Engineering and Materials Science, Soochow University, Suzhou, 215123, P. R. China

[‡]Department of Polymer Chemistry and Biomaterials, Faculty of Science and Technology, MIRA Institute for Biomedical Technology and Technical Medicine, University of Twente, P.O. Box 217, 7500 AE Enschede, The Netherlands

ABSTRACT: Pyridyl disulfide-functionalized cyclic carbonate (PDSC) monomer was obtained in four straightforward steps from 3-methyl-3-oxetanemethanol and exploited for facile preparation of functional poly(ε-caprolactone) (PCL) containing pendant pyridyl disulfide (PDS) groups via ring-opening copolymerization with ε-caprolactone. The results showed that PDS-functionalized PCL polymers were prepared with controlled molecular weights and functionalities. The exchange reaction between PDS-functionalized PCL and thiolated poly(ethylene glycol) (PEG-SH) at a PEG-SH/PDS molar ratio of 2/1 afforded PCL-*g*-SS-PEG graft copolymers in high yields. The dynamic light scattering (DLS) analyses showed that PCL-*g*-SS-PEG copolymer self-assembled into micelles with a diameter of 110−120 nm and a low polydispersity (PDI) in phosphate buffer (pH 7.4, 10 mM). PCL-*g*-SS-PEG micelles while sufficiently stable under physiological conditions were prone to rapid shell shedding and aggregation under a reductive condition. Doxorubicin (DOX) was loaded into PCL-*g*-SS-PEG micelles with a decent drug loading content of 10.1 wt %. Notably, *in vitro* release studies revealed that ca. 82.1% DOX was released in 12 h under a reductive environment analogous to that of the intracellular compartments such as cytosol and the cell nucleus whereas only ca. 17.5% DOX was released in 24 h under nonreductive conditions. Confocal microscopy observation indicated that DOX was delivered into the nuclei of HeLa cells following 8 h incubation with DOX-loaded PCL-*g*-SS-PEG micelles. MTT assays in HeLa cells demonstrated that DOX-loaded PCL-*g*-SS-PEG micelles retained high antitumor activity with low IC_{50} (half-maximal inhibitory concentration) of 0.82−0.95 μg DOX equiv/mL while blank PCL-*g*-SS-PEG micelles were nontoxic up to a tested concentration of 1.0 mg/mL. This study presents a versatile and controlled synthesis of PDS-functionalized biodegradable polymers and reduction-sensitive biodegradable graft copolymer micelles that are of particular interest for active intracellular drug release.

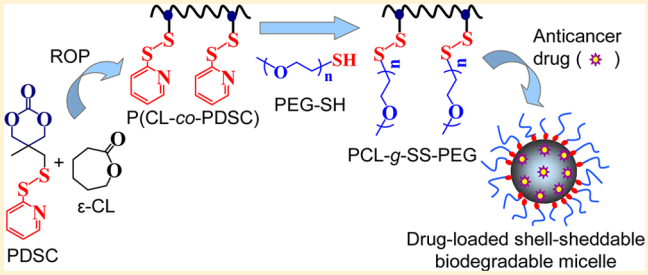

INTRODUCTION

Aliphatic polyesters and polycarbonates, such as poly(ε-caprolactone) (PCL), polylactide (PLA), poly(lactide-*co*-glycolide) (PLGA), and poly(trimethylene carbonate) (PTMC), are among the most important synthetic biodegradable materials.[1−3] They have been widely applied for absorbable orthopedic devices,[4] microparticles for controlled protein release,[5,6] cell and tissue scaffolds,[7,8] drug-eluting stents,[9] and nanoparticles for targeted and controlled drug release.[10,11] However, these traditional biodegradable polymers are lack of reactive groups, which renders them difficult to develop advanced drug delivery systems and bioactive tissue scaffolds. In the past decade, various functional aliphatic polyesters and polycarbonates with pendant hydroxyl,[12,13] carboxyl,[14,15] amine,[16,17] allyl,[18−20] alkyne/azide,[21−24] acryloyl,[25−27] and maleimide[28] groups have been reported. In particular, design of functional cyclic carbonate monomers has received recent interest.[29,30] We have designed 2,4,6-trimethoxybenzylacetal, (methyl)acryloyl, or vinyl sulfone-functionalized cyclic carbonate monomers that provided versatile access to pH-sensitive degradable micelles and polymersomes,[31,32] photo-cross-linked biodegradable micelles,[33−35] biodegradable injectable hydrogels,[36] and functional biodegradable polymers and coatings.[37]

In recent years, taking advantage of high redox potential in the cytoplasms and nuclei of cancer cells, reduction-sensitive degradable micelles and nanoparticles have been actively

Received: December 5, 2012
Revised: January 17, 2013
Published: January 30, 2013

Scheme 1. Synthesis of Functional PCL Containing Pendant Pyridyl Disulfide Groups and Facile Access to Reduction-Sensitive Biodegradable Graft Copolymer Micelles for Intracellular Drug Release

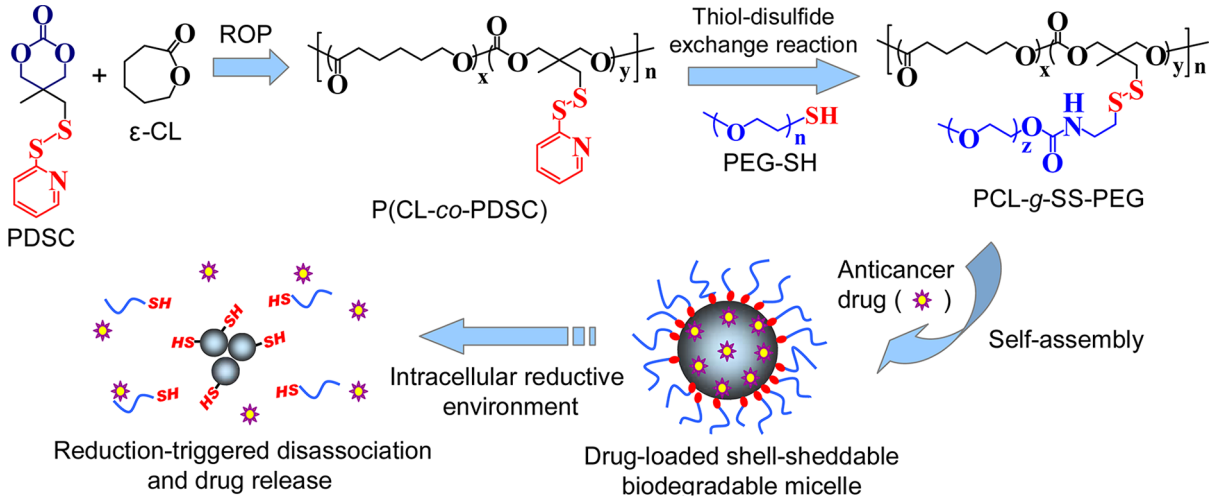

developed for efficient intracellular anticancer drug release.[38,39] The intracellular doxorubicin (DOX) level and antitumor activity of DOX-loaded reduction-sensitive shell-sheddable micelles were significantly enhanced as compared to reduction-insensitive controls. It should be noted that pyridyl disulfide (PDS) is the most versatile thiol−disulfide exchange functional group used for the construction of disulfide linkages and cross-links in bioconjugate chemistry.[40] For example, Hoffman et al. designed poly(methacrylic acid-*co*-butyl acrylate-*co*-pyridyl disulfide acrylate) random copolymer for facile conjugation and active intracellular release of thiol-containing therapeutic oligopeptide drugs.[41] Thayumanavan et al. developed reduction-responsive polymeric nanogels based on a random copolymer containing oligoethylene glycol and PDS units as side-chain functionalities, in which PDS was used to form disulfide cross-links as well as to introduce TAT peptide or FITC on nanogel surfaces.[42,43]

In this paper, we report synthesis of novel functional PCL via ring-opening copolymerization of ε-CL and pyridyl disulfide-functionalized cyclic carbonate (PDSC) monomer (Scheme 1). The postpolymerization modification with thiolated PEG by thiol−disulfide exchange reaction yielded reduction-sensitive, amphiphilic, biodegradable graft copolymers that are self-assembled into stable micellar nanoparticles in water. It is interesting to note that graft copolymer micelles offer several advantages over block copolymer micelles; for instance, they often exhibit enhanced stability with low critical micelle concentration (cmc),[44−46] micellar core and surface properties can be broadly adjusted by backbone length, graft density, and graft length, and presence of many hydrophilic grafts per macromolecule enables conjugation of tunable density targeting ligands for optimal tumor targeting. However, there are few reports on biodegradable graft copolymer micelles based on hydrophobic biodegradable polymers grafted with hydrophilic polymers,[21,44,47] likely due to challenging synthesis. In this study, synthesis and ring-opening copolymerization of PDSC monomer, synthesis and self-assembly of PCL-*g*-SS-PEG graft copolymer, loading and reduction-responsive release of DOX, and intracellular release and antitumor activity of DOX-loaded graft copolymer micelles were investigated.

EXPERIMENTAL SECTION

Materials. 3-Methyl-3-oxetanemethanol (97%, Alfa), hydrobromic acid (40%, SCRC), sodium hydrosulfide hydrate (68%, Acros), 2,2′-dipyridyl disulfide (98%, Alfa Aesar), triethylamine (Et_3N, Alfa Aesar, 99%), stannous octoate ($Sn(Oct)_2$, 95%, Sigma), and doxorubicin hydrochloride (DOX·HCl, 99%, Beijing Zhong Shuo Pharmaceutical Technology Development Co. Ltd.) were used as received. ε-Caprolactone (ε-CL, 99%, Alfa Aesar) was dried over CaH_2 and distilled under reduced pressure prior to use. Thiolated PEG (PEG-SH, M_n = 5.0 kg/mol) was synthesized according to a previous report.[48] Tetrahydrofuran (THF) and toluene were dried by refluxing over sodium wire under an argon atmosphere prior to distillation. Isopropanol was dried by refluxing over CaH_2 under an argon atmosphere. Ethyl chloroformate was freshly distilled before use.

Preparation of Pyridyl Disulfide Carbonate (PDSC). Pyridyl disulfide carbonate (PDSC) was synthesized in four steps (Scheme 1). The first two steps were carried out according to our previous report.[37] Briefly, HBr (40%, 40 mL) was dropwise added into a solution of 3-methyl-3-oxetanemethanol (10.20 g, 100.0 mmol) in THF (100 mL) under stirring at 0 °C. The reaction mixture was warmed to room temperature and stirred for another 5 h. The reaction mixture was then diluted with H_2O (150 mL) and extracted with diethyl ether (4 × 150 mL). The organic phase was dried over anhydrous $MgSO_4$ and concentrated to give the desired product (bromo-diol) as a white solid. Yield: 17.57 g (96%). ^{1}H NMR (400 MHz, $CDCl_3$): δ 3.68 (s, 4H, $-C(CH_2OH)_2$), 3.55 (s, 2H, $-CH_2Br$), 2.13 (s, 2H, $-(OH)_2$), 0.93 (s, 3H, $-CH_3$).

Next, bromo-diol (9.15 g, 50.0 mmol) was added under stirring to a solution of NaSH (8.40 g, 150.0 mmol) in DMF (150 mL). The reaction mixture was stirred at 75 °C for 20 h. The solvent was removed by rotary evaporation, the residue was dissolved in 150 mL of deionized water and extracted with ethyl acetate (3 × 150 mL), and the organic phase was dried over anhydrous $MgSO_4$ and concentrated to yield mercapto-diol as a yellowish oil. Yield: 3.54 g (52%). ^{1}H NMR (400 MHz, $CDCl_3$): δ 3.64 (d, 4H, $-C(CH_2OH)_2$), 2.67 (d, 2H, $-CH_2SH$), 2.27 (s, 2H, $-(OH)_2$), 1.31 (t, 1H, $-SH$), 0.85 (s, 3H, $-CH_3$).

Then, to a stirred solution of 2,2′-dithiodipyridine (8.68 g, 39.0 mmol) and a catalytic amount of glacial acetic acid (0.5 mL) in methanol (75 mL) was added dropwise a solution of mercapto-diol (3.54 g, 26.0 mmol) in methanol at room temperature. The reaction mixture was stirred at room temperature for an additional 16 h. The solvent was evaporated to yield crude product as a yellow oil. The product was purified by column chromatography using silica gel as stationary phase and a mixture of ethyl acetate/petroleum ether (v/v = 1/3) as eluent. Yield: 4.14 g (65%). ^{1}H NMR (400 MHz, $CDCl_3$): δ

dx.doi.org/10.1021/ma302499a | *Macromolecules* 2013, 46, 699−707

8.47, 7.62, 7.41, and 7.17 (m, pyridyl protons), 3.67 (d, 4H, $-C(CH_2OH)_2$), 3.25 (s, 2H, $-CH_2SS$-Py), 0.84 (s, 3H, $-CH_3$).

Finally, to a stirred solution of pyridyl disulfide-diol (4.14 g, 16.9 mmol) and ethyl chloroformate (3.4 mL, 35.5 mmol) in dried THF (150 mL) at 0 °C was added dropwise a solution of Et_3N (5.4 mL, 39.1 mmol) in THF. The reaction was allowed to proceed for 4 h at 0 °C. The reaction mixture was filtered, the filtrate was concentrated under reduced pressure, and the residues were crystallized in THF/diethyl ether to yield a white solid. Yield: 3.66 g (50%). ^{1}H NMR (400 MHz, $CDCl_3$): δ 8.51, 7.65, 7.54, and 7.14 (m, pyridyl protons), 4.38–4.15 (d, 4H, $-C(CH_2O)_2CO$), 3.08 (s, 2H, $-CH_2SS$-Py), 1.23 (s, 3H, $-CH_3$). Elemental Analysis: Calcd for $C_9H_{12}O_5$: C, 48.69; N, 5.16; H, 4.83. Found C, 48.70; N, 5.02; H, 4.75. TOF-MS (m/z): calcd for $C_{11}H_{13}NO_3S_2$ 271.36; found 271.37.

Ring-Opening Copolymerization. The ring-opening copolymerization of ε-CL and PDSC was carried out in toluene at 100 °C using isopropanol as an initiator and $Sn(Oct)_2$ as a catalyst. The following is a typical example. In a glovebox under a nitrogen atmosphere, to a stirred solution of ε-CL (0.757 g, 6.64 mmol) and PDSC (0.200 g, 0.74 mmol) in toluene (8 mL) was quickly added isopropanol stock solution (0.18 mL, 0.2 M) and $Sn(Oct)_2$ stock solution (0.20 mL, 100 mM). The reaction vessel was sealed and placed in an oil bath thermostated at 100 °C with magnetic stirring for 24 h. A sample was taken for determination of the monomer conversion using ^{1}H NMR. The resulting P(CL-*co*-PDSC) copolymer was isolated by precipitation in cold diethyl ether and dried *in vacuo* at room temperature.

Synthesis of PCL-*g*-SS-PEG by Thiol–Disulfide Exchange Reaction. To a solution of P(CL-*co*-PDSC) 5.4% (50 mg, 20 μmol of PDS groups) and PEG-SH (200 mg, 40 μmol) in DCM under a nitrogen atmosphere was added a catalytic amount of acetic acid. The reaction was allowed to proceed with stirring for 48 h at room temperature. The resulting polymer was isolated by precipitation from cold diethyl ether, washed with excess ethanol, and dried *in vacuo* at room temperature.

Characterization. ^{1}H NMR spectra were recorded on the Unity Inova 400 operating at 400 MHz. $CDCl_3$ was used as solvent and the chemical shifts were calibrated against residual solvent signals. The molecular weight and polydispersity of the copolymers were determined by a Waters 1515 gel permeation chromatograph (GPC) instrument equipped with two linear PLgel columns (500 Å and Mixed-C) following a guard column and a differential refractive index detector. The measurements were performed using $CHCl_3$ as the eluent at a flow rate of 0.5 mL/min at 30 °C and a series of narrow polystyrene standards for the calibration of the columns.

Micelle Formation and Critical Micelle Concentration. Micelles were typically prepared under stirring by dropwise addition of 2 mL of phosphate buffer (10 mM, pH 7.4) to 0.2 mL of amphiphilic PCL-*g*-SS-PEG copolymer solution (0.5 wt %) in THF at room temperature. The resulting solution was stirred overnight under reduced pressure to allow complete evaporation of THF. The size and size distribution of the micelles were determined by dynamic light scattering (DLS). The micellar suspension was filtered through a 450 nm syringe filter before measurements. Measurements were carried out at 25 °C using a Zetasizer Nano-ZS from Malvern Instruments equipped with a 633 nm He–Ne laser using backscattering detection.

The critical micelle concentration (cmc) was determined using pyrene as a fluorescence probe. The concentration of graft copolymer was varied from 2.0×10^{-5} to 0.2 mg/mL, and the concentration of pyrene was fixed at 1.0 μM. Fluorescence spectra were recorded using a FLS920 fluorescence spectrometer and an excitation wavelength of 330 nm. Fluorescence emissions at 372 and 383 nm were monitored. The cmc was estimated as the cross-point when extrapolating the intensity ratio I_{372}/I_{383} at low and high concentration regions.

Redox-Triggered Change of Micelle Sizes. The change in size, size distribution, and light scattering of the micelles in response to 10 mM DTT was followed by DLS at 37 °C. The micelles were prepared as above. PCL-*g*-SS-PEG micellar suspension (0.2 mg/mL) was divided into two aliquots. To one of the aliquots (1.0 mL) was added 10 μL of DTT (1.0 M), which gave a final DTT concentration of 10 mM. The samples were gentlely stirred at 37 °C. The changes in micelle size and PDI were monitored over time by DLS.

Loading and Redox-Triggered Release of DOX. DOX was loaded into micelles by dropwise addition of 2 mL of phosphate buffer (10 mM, pH 7.4) to a mixture of 0.2 mL of copolymer solution in DMF (5 mg/mL) and 10, 20, or 40 μL of DOX solution in DMSO (5 mg/mL) under stirring at room temperature, followed by stirring for 1 h and dialysis against phosphate buffer (10 mM, pH 7.4) with a molecular weight cutoff (MWCO) of 3500 Da at room temperature in the dark for 6 h.

The release profiles of DOX from PCL-*g*-SS-PEG micelles were studied using a dialysis tube (MWCO 12 000 Da) at 37 °C in two different media, i.e., PB (100 mM, pH 7.4) or PB (100 mM, pH 7.4) with 10 mM DTT. In order to acquire sink conditions, drug release studies were performed at low drug loading contents (ca. 2.9 wt %) and with 0.6 mL of micelle suspension dialysis against 20 mL of the same medium. At desired time intervals, 5.0 mL of release media was taken out and replenished with an equal volume of fresh media. The amount of DOX released was determined by using fluorescence (FLS920) measurement (excitation at 480 nm). The release experiments were conducted in triplicate. The results presented are the average data. For determination of the drug loading content, DOX-loaded micellar suspensions were freeze-dried, then dissolved in DMSO, and analyzed with fluorescence spectroscopy. A calibration curve was obtained using DOX/DMSO solutions with different DOX concentrations. To determine the amount of DOX released, calibration curves were run with DOX/phosphate buffer solution (pH 7.4, 100 mM) with different DOX concentrations. The emission at 600 nm was recorded. Release experiments were conducted in triplicate. The results are presented as the average ± standard deviation.

Drug loading content (DLC) and drug loading efficiency (DLE) were calculated according to the following formulas:

$$\text{DLC (wt \%)} = \frac{\text{weight of loaded drug}}{\text{total weight of polymer and loaded drug}} \times 100\%$$

$$\text{DLE (\%)} = \frac{\text{weight of loaded drug}}{\text{weight of drug in feed}} \times 100\%$$

Confocal Microscopy Observation of HeLa Cells Incubated with DOX-Loaded Micelles. HeLa cells were plated on microscope slides in a 24-well plate (5×10^4 cells/well) using DMEM medium containing 10% FBS. The cells were incubated with prescribed amounts of DOX-loaded PCL-*g*-SS-PEG **2** micelles or free DOX at 37 °C and 5% CO_2. After incubation for 4 and 8 h, the culture medium was removed and the cells on microscope plates were washed three times with PBS. The cells were fixed with 4% paraformaldehyde, and the cell nuclei were stained with DAPI. Fluorescence images of cells were obtained with a Nikon Digital Eclipse C1si confocal laser scanning microscope (CLSM, Nikon).

MTT Assays. The cytotoxicity of PCL-*g*-SS-PEG micelles and DOX-loaded PCL-*g*-SS-PEG micelles was studied by MTT assays using HeLa cells. Cells were seeded onto a 96-well plate at a density of 1×10^4 cells per well in 100 μL of Dulbecco's Modified Eagle medium (DMEM) containing 10% FBS and incubated for 24 h (37 °C, 5% CO_2). The medium was replaced by 90 μL of fresh DMEM medium containing 10% FBS, and then 10 μL samples of various concentrations (0.5–10 mg/mL) of the micelle suspensions in phosphate buffer (10 mM, pH 7.4) were added. The cells were incubated for another 48 h, the medium was aspirated and replaced by 100 μL of fresh medium, and 10 μL of MTT solution (5 mg/mL) was added. The cells were incubated for 4 h, and then the medium was aspirated and replaced by 150 μL of DMSO to dissolve the resulting purple crystals. The optical densities at 570 nm were measured using a BioTek microplate reader. Cells cultured in DMEM medium containing 10% FBS (without exposure to micelles) were used as controls.

dx.doi.org/10.1021/ma302499a | *Macromolecules* 2013, 46, 699–707

RESULTS AND DISCUSSION

Synthesis of PDSC Monomer. Pyridyl disulfide-functionalized cyclic carbonate (PDSC) was prepared in four straightforward steps: (i) 3-methyl-3-oxetanemethanol was treated with HBr to afford bromo-diol; (ii) bromo-diol was reacted with sodium hydrosulfide to yield mercapto-diol; (iii) thiol-exchange reaction between mercapto-diol and excess 2,2′-dipyridyl disulfide gave rise to pyridyl disulfide-diol; and (iv) similar to reported procedure for other cyclic carbonate monomers[27,31] cyclization of pyridyl disulfide-diol using ethyl chloroformate in dilute anhydrous THF solution at 0 °C with dropwise addition of triethylamine furnished PDSC monomer in decent yields (Scheme 2). PDSC monomer could be readily

Scheme 2. Synthetic Pathway for Pyridyl Disulfide-Functionalized Cyclic Carbonate Monomer (PDSC)[a]

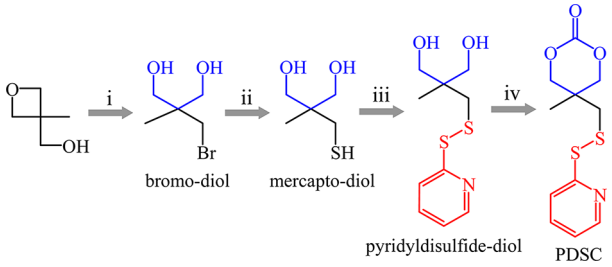

[a]Conditions: (i) 40% hydrobromic acid, 0 °C, 5 h, THF (yield 96%); (ii) sodium hydrosulfide, 75 °C, overnight, DMF (yield 52%); (iii) 2,2′-dithiodipyridine, catalytic amount of glacial acetic acid, room temperature, overnight, methanol (yield 65%); (iv) ethyl chloroformate, Et_3N, 0 °C, 4 h, THF (yield 50%).

recrystallized from dry THF/diethyl ether to yield pure white crystals. ^{1}H NMR spectrum of pyridyl disulfide-diol showed signals of pyridine protons at δ 8.47, 7.62, 7.41 and 7.17 as well as resonances at δ 3.67, 3.25, and 0.84 attributable to methylene protons next to hydroxyl groups, methylene protons neighboring the disulfide bond, and methyl protons, respectively (Figure 1A). ^{1}H NMR of PDSC revealed that signals assignable to the methylene protons next to the carbonate were clearly detected

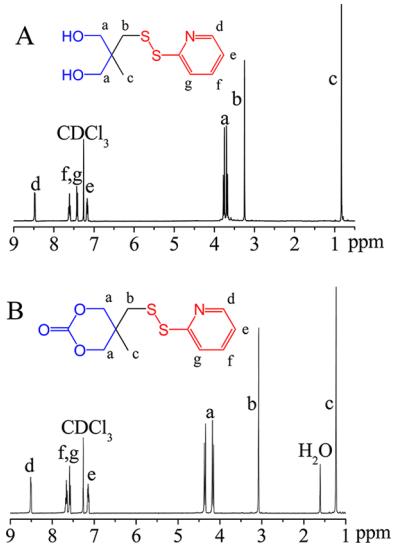

Figure 1. ^{1}H NMR spectra (400 MHz, $CDCl_3$) of pyridyl disulfide-diol (A) and PDSC monomer (B).

at δ 4.15−4.38 while signals at δ 3.67 owing to methylene protons next to hydroxyl groups shifted to δ 4.15−4.38 (Figure 1B). The integral ratio of resonances at δ 4.15−4.38 and δ 8.51, 7.65, 7.54, and 7.14 (pyridine protons) was close to the theoretical value of 1:1, indicating successful synthesis of PDSC monomer. The structure of PDSC was further confirmed by mass and elemental analyses. Hedrick et al. reported versatile synthesis of functionalized cyclic carbonate monomers through a pentafluorophenyl ester intermediate, which reacting with *S*-2-pyridyl-*S*′-2-hydroxyethyl disulfide could yield 2-(pyridin-2-yl-disulfanyl)ethyl 5-methyl-2-oxo-1,3-dioxane-5-carboxylate.[49] However, ring-opening (co)polymerization of pyridyl disulfide-functionalized carbonate monomer to synthesize biodegradable polymers with pendant PDS groups and further reduction-sensitive amphiphilic biodegradable graft copolymers has not yet been reported.

Synthesis of Functional PCL Containing Pendant PDS Groups. The aim of this study was to provide a versatile approach to PDS-functionalized biodegradable polymers and reduction-sensitive biodegradable graft copolymers by post-polymerization modification with thiol-containing molecules. To prove our concept, we synthesized PDS-functionalized PCL as an example (Scheme 3). The results showed that PDSC was readily copolymerized with ε-CL in toluene at 100 °C using isopropanol as an initiator and $Sn(Oct)_2$ as a catalyst to afford PDS-functionalized PCL in good yields (Table 1). ^{1}H NMR showed that signals characteristic of both CL units (δ 4.04, 2.30, 1.64, and 1.38) and PDSC units (δ 8.46, 7.65, 7.10, 4.05, 3.02, and 1.10) were clearly detected (Figure 2). Importantly, signals due to pyridine protons maintained at δ 8.46, 7.65, and 7.10, indicating that PDS functional groups were intact during copolymerization and subsequent work-up procedures. The copolymer compositions could be determined by comparing signals at δ 2.30 (methylene protons next to carbonyl in CL units) and 3.02 (methylene protons next to disulfide bond in PDSC units). The results showed that P(CL-*co*-PDSC) copolymers with PDSC contents (F_{PDSC}) ranging from 2.5 to 10.3 mol % were obtained at PDSC monomer feed ratio (f_{PDSC}) varying from 5 to 20 mol % (Table 1). F_{PDSC} though lower than feed ratios increased linearly with increasing f_{PDSC}, denoting good control over PDS functionality. The number-average molecular weights (M_n) estimated from ^{1}H NMR end-group analysis by comparing the integrals of peaks at 2.30 (methylene protons next to carbonyl in CL units) and 3.02 (methylene protons next to disulfide bond in PDSC units) with δ 1.22 (methyl protons of isopropyl ester end group) were close to the theoretical values (Table 1). Gel permeation chromatography (GPC) measurements using polystyrene as standards showed that these P(CL-*co*-PDSC) copolymers had moderate polydispersities (PDI) of 1.33−1.61 and M_n increased with increasing monomer-to-initiator ratios (Table 1). Therefore, copolymerization of ε-CL and PDSC provides PDS-functionalized PCL with controlled molecular weights and functionalities.

Synthesis of PCL-*g*-SS-PEG Graft Copolymer by Thiol−Disulfide Exchange Reaction. It is well-known that the pyridyl disulfide group has a high reactivity toward thiol-containing molecules via thiol−disulfide exchange reaction to form disulfide linkages or cross-links.[50] Here, two P(CL-*co*-PDSC) copolymers with similar PDS functionality (5.2−5.4%) but different M_n values (12.6 and 22.3 kg/mol; Table 1, entries 2 and 4) were chosen to react with thiolated PEG (M_n = 5000). The reaction was performed at a PEG-SH/PDS molar ratio of

dx.doi.org/10.1021/ma302499a | *Macromolecules* 2013, 46, 699−707

Scheme 3. Synthesis of P(CL-*co*-PDSC) Copolymer and Reduction-Sensitive PCL-*g*-SS-PEG Graft Copolymer[a]

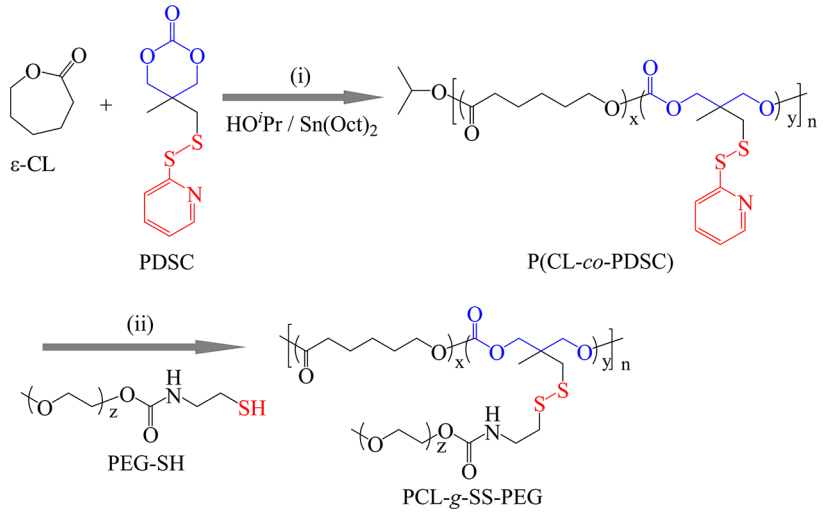

[a]Conditions: (i) ring-opening copolymerization of ε-CL and PDSC using isopropanol as an initiator and Sn(Oct)$_2$ as a catalyst in toluene at 100 °C; (ii) thiol−disulfide exchange reaction with thiolated PEG using catalytic amount of acetic acid in DCM at room temperature.

Table 1. Synthesis of Pyridyl Disulfide-Functionalized PCL[a]

				M_n (×10^3)			
entry	[M]/[I]	f^b (%)	F^c (%)	design	^{1}H NMR^d	GPC^e	PDI GPC^e
1	100	5	3.2	12.2	12.0	18.6	1.42
2	100	10	5.2	13.0	12.6	19.2	1.40
3	200	5	2.5	24.4	20.1	30.9	1.55
4	200	10	5.4	25.9	22.3	29.6	1.52
5	200	20	10.3	29.1	21.4	29.8	1.33
6	400	5	2.7	44.7		55.5	1.61

[a]The copolymerization was carried out in toluene at 100 °C using isopropanol as an initiator and Sn(Oct)$_2$ as a catalyst at a total monomer-to-initiator ratio of 100/1, 200/1, and 400/1. [b]Molar fraction of PDSC monomer in feed. [c]Molar fraction of PDSC units in the resulting copolymer determined by ^{1}H NMR. [d]Estimated by ^{1}H NMR end-group analysis. [e]Determined by GPC (eluent: chloroform; flow rate: 0.5 mL/min; standards: polystyrene).

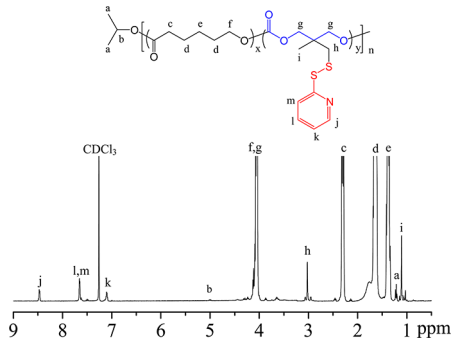

Figure 2. ^{1}H NMR spectrum (400 MHz, CDCl$_3$) of P(CL-*co*-PDSC) copolymer (Table 1, entry 4).

2/1 in DCM at room temperature for 48 h using a catalytic amount of acetic acid (Scheme 3). The free PEG was removed by washing with excess ethanol. ^{1}H NMR displayed that new signals corresponding to methylene protons of PEG appeared at δ 3.65 while peaks due to pyridine groups at δ 8.46, 7.65 and 7.10, were diminishing (Figure 3). The comparison of integrals of resonances at δ 3.36 (methoxyl protons of PEG) and δ 1.02

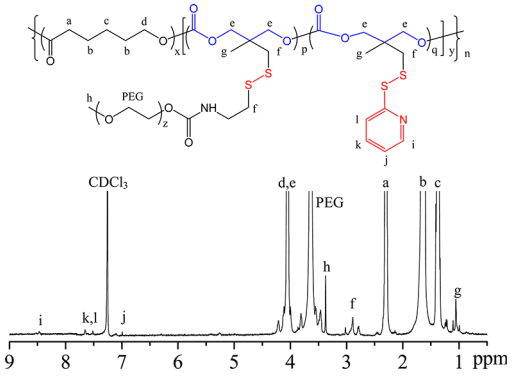

Figure 3. ^{1}H NMR spectrum (400 MHz, CDCl$_3$) of PCL-*g*-SS-PEG copolymer (Table 2, entry 2).

(methyl protons of PDSC units) indicated that ca. 86−89% pyridyl disulfide groups have reacted with thiolated PEG to afford amphiphilic PCL-*g*-SS-PEG graft copolymers (Table 2). The M_n of these two copolymers was calculated by ^{1}H NMR to be 35.6 and 66.0 kg/mol (denoted as PCL-*g*-SS-PEG **1** and **2**, respectively). GPC curves of both graft copolymers remained unimodal with a PDI of 1.95−2.02 (Table 2). The M_n determined by GPC was lower than that calculated from ^{1}H NMR, likely due to their graft structure. The deviation of M_n could be also partly because polystyrene was used as a standard for GPC measurements. It is evident that PCL-*g*-SS-PEG graft copolymers can be readily prepared from PDS-functionalized PCL via thiol−disulfide exchange reaction.

Formation and Reduction-Triggered Disruption of Micelles. Micelles of PCL-*g*-SS-PEG copolymers were prepared by the solvent exchange method. Dynamic light scattering (DLS) measurements showed that PCL-*g*-SS-PEG copolymers formed micelles with average sizes of 110−120 nm and low polydispersities (PDIs) of 0.09−0.12 (Figure 4A). The critical micelle concentration (cmc) was determined using pyrene as a probe in 10 mM PB at pH 7.4 (Figure 4B). The results showed that PCL-*g*-SS-PEG **1** and **2** had particularly low cmc of 0.92 and 0.87 mg/L, respectively (Table 2), supporting

dx.doi.org/10.1021/ma302499a | *Macromolecules* 2013, 46, 699−707

Table 2. Synthesis of PCL-*g*-SS-PEG Graft Copolymer

	P(CL-*co*-PDSC)			M_n ($\times 10^3$)			
PCL-*g*-SS-PEG copolymer	F_{PDSC} (%)	M_n ($\times 10^3$)	PEG conjugation[a] (%)	^{1}H NMR[b]	GPC[c]	PDI GPC[c]	cmc[d] (mg/L)
1	5.2	12.6	86	35.6	28.6	2.02	0.92
2	5.4	22.3	89	66.0	43.9	1.95	0.87

[a]Percentage of PEG conjugation determined by ^{1}H NMR. [b]Determined by ^{1}H NMR according to the integral ratio of resonances at δ 3.36 (methoxyl protons attributed to PEG) and δ 1.02 (methyl protons attributed to initial PDSC units). [c]Determined by GPC (eluent: chloroform; flow rate: 0.5 mL/min; standards: polystyrene). [d]Critical micelle concentration (cmc) determined using pyrene as fluorescence probe.

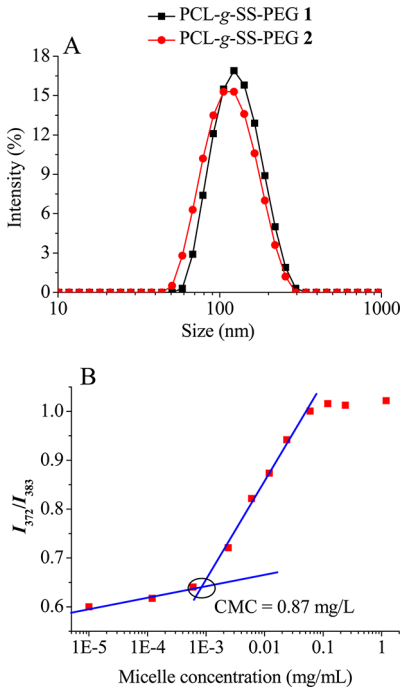

Figure 4. Size distribution of PCL-*g*-SS-PEG graft copolymer micelles determined by DLS (A) and the fluorescence intensity ratio I_{372}/I_{383} of pyrene as a function of PCL-*g*-SS-PEG **2** concentration (B).

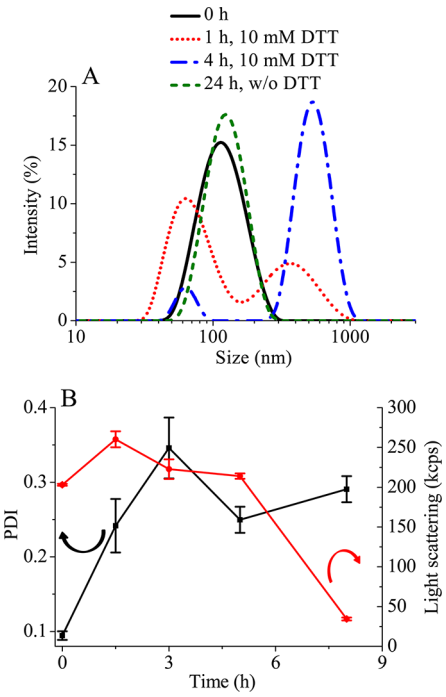

Figure 5. Change of particle sizes (A) and PDI and light scattering intensity (B) of PCL-*g*-SS-PEG **2** micelles in time in response to 10 mM DTT.

that amphiphilic graft copolymers form particularly stable micelles.

The reduction-sensitive property of PCL-*g*-SS-PEG **2** micelles was studied using DLS by monitoring change of micelle sizes in response to 10 mM dithiothreitol (DTT) in PB buffer (pH 7.4, 10 mM). The results showed that micelles were quickly destabilized by DTT to form large aggregates of about 600 nm in 4 h (Figure 5A), accompanied by decrease of light scattering intensity and increase of PDI (Figure 5B). These results are in line with our previous observations for PEG-SS-PCL micelles.[48] In contrast, no change in micelle sizes and PDIs was discerned after 24 h in the absence of DTT under otherwise the same conditions. DTT-triggered cleavage of disulfide bonds in PCL-*g*-SS-PEG **2** micelles was also confirmed by GPC in that PCL-*g*-SS-PEG **2** micelles following treatment with DTT gave two distributions corresponding to P(CL-*co*-PDSC) copolymer (Table 1, entry 4) and PEG, respectively.

Loading and Triggered Release of DOX. DOX was loaded into PCL-*g*-SS-PEG micelles at theoretical drug loading contents (DLC) of 4.8, 9.1, and 16.7 wt %. Interestingly, PCL-*g*-SS-PEG **1** and **2** micelles exhibited similar DOX loading levels and particles sizes (Table 3), indicating that molecular weights of amphiphilic graft copolymers have little influences on drug loading behaviors. The drug loading efficiencies (DLE) ranged from 54.1 to 71.1%, which decreased with increasing DLC.

Table 3. DOX Loading Content and Loading Efficiency of Polymeric Micelles

	DLC (wt %)				
polymer	theory	determined[a]	DLE (%)	size (nm)	PDI
PCL-*g*-SS-PEG **1**	4.8	3.3 ± 0.07	68.2 ± 1.5	56.2 ± 0.5	0.13
	9.1	5.7 ± 0.09	60.3 ± 1.6	68.7 ± 1.5	0.17
	16.7	9.8 ± 0.12	54.1 ± 2.0	116.1 ± 2.6	0.23
PCL-*g*-SS-PEG **2**	4.8	3.4 ± 0.06	71.1 ± 1.4	58.9 ± 0.4	0.12
	9.1	5.8 ± 0.09	61.5 ± 1.7	64.8 ± 1.3	0.14
	16.7	10.1 ± 0.13	55.9 ± 2.1	108.2 ± 2.1	0.20

[a]Drug loading content for DOX was determined by fluorescence measurements.

Moreover, DOX-loaded PCL-*g*-SS-PEG micelles had low PDIs of 0.12−0.23 and particle sizes ranging from 56.2 to 116.1 nm depending on DOX loading levels. The micelle size became smaller at a low drug loading level likely due to existence of effective interactions between micellar core and DOX.

The *in vitro* release of DOX from PCL-*g*-SS-PEG **2** micelles was investigated using a dialysis tube (MWCO 12 000 Da) in PB buffer (pH 7.4, 100 mM) at 37 °C in either the presence or absence of 10 mM DTT. Interestingly, the results showed that

dx.doi.org/10.1021/ma302499a | *Macromolecules* 2013, 46, 699−707

DOX was released rapidly in response to 10 mM DTT, in which ca. 62.1% and 82.0% DOX was released in 4 and 12 h, respectively (Figure 6). In contrast, minimal drug release (ca.

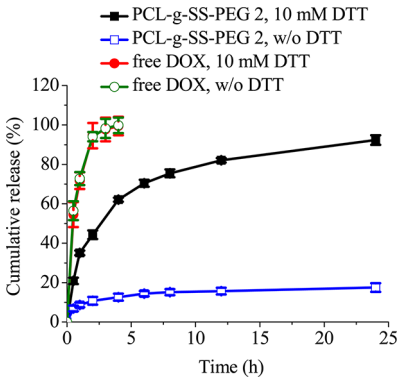

Figure 6. Reduction-triggered release of DOX from PCL-*g*-SS-PEG **2** micelles in phosphate buffer (pH 7.4, 100 mM). The release of free DOX was used as a control.

17.5%) was observed within 24 h in the absence of 10 mM DTT under otherwise the same conditions. This redox-triggered drug release behavior has been reported for various shell-sheddable micelles.[48,51−54] This fast drug release is likely because micelles following shedding of PEG shells are destabilized and form drug diffusion channels. These reduction-sensitive biodegradable graft copolymer micelles with easy synthesis, enhanced stability, and redox-triggered rapid drug release behaviors are highly interesting as "smart" vehicles for active intracellular drug release.

Intracellular Drug Release and Antitumor Activity of DOX-Loaded PCL-*g*-SS-PEG Micelles. The cellular uptake and intracellular drug release behaviors of DOX-loaded PCL-*g*-SS-PEG micelles were studied using CLSM. The cell nuclei were stained with DAPI (blue). Interestingly, the results showed that DOX-loaded PCL-*g*-SS-PEG micelles delivered and released DOX into the perinuclei and nuclei regions following 4 h incubation (Figure 7A), indicating fast internalization of micelles and rapid release of DOX inside cells. At a longer incubation time of 8 h, DOX was fully delivered into the nuclei of HeLa cells (Figure 7B). It is remarkable to note that DOX-loaded PCL-*g*-SS-PEG micelles displayed a similar intracellular DOX release rate to free DOX (Figure 7C).

MTT assays revealed that both PCL-*g*-SS-PEG **1** and **2** micelles were nontoxic to HeLa cells with cell viabilities more than 98% up to a tested concentration of 1.0 mg/mL (Figure 8A), confirming that these biodegradable graft copolymer micelles have excellent biocompatibility. DOX-loaded PCL-*g*-SS-PEG micelles, however, displayed pronounced antitumor activity toward HeLa cells following 48 h incubation (Figure 8B). DOX-loaded PCL-*g*-SS-PEG **1** and **2** micelles had low IC_{50} (half-maximal inhibitory concentration) of 0.95 and 0.82 μg DOX equiv/mL, respectively, which was close to that observed for free DOX (IC_{50} = 0.46 μg/mL). It should further be noted that the antitumor activity of graft copolymer micellar drugs could further be enhanced by installing a tumor-targeting ligand like aptamer, peptide, and antibody fragment that facilitates efficient and specific tumor cell uptake of micelles. These redox-sensitive biodegradable graft polymer micelles with excellent biocompatibility, low cmc, and intracellular redox-responsive drug release are highly promising for targeted cancer therapy.

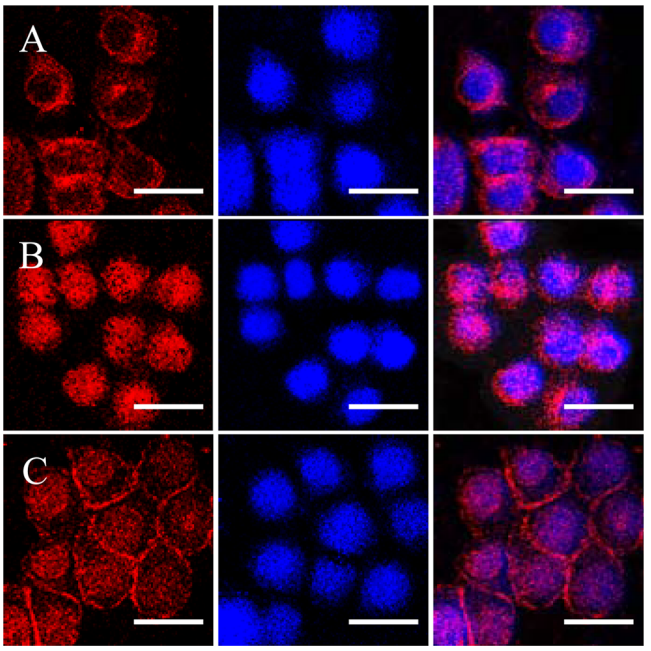

Figure 7. CLSM images of HeLa cells following 4 or 8 h incubation with DOX-loaded PCL-*g*-SS-PEG **2** micelles and free DOX (10 μg/mL). For each panel, the images from left to right showed cell nuclei stained by DOX fluorescence in cells (red), DAPI (blue), overlays of both images. The scale bars correspond to 25 μm in all the images. (A) DOX-loaded PCL-*g*-SS-PEG **2** micelles, 4 h; (B) DOX-loaded PCL-*g*-SS-PEG **2** micelles, 8 h; (C) free DOX, 4 h.

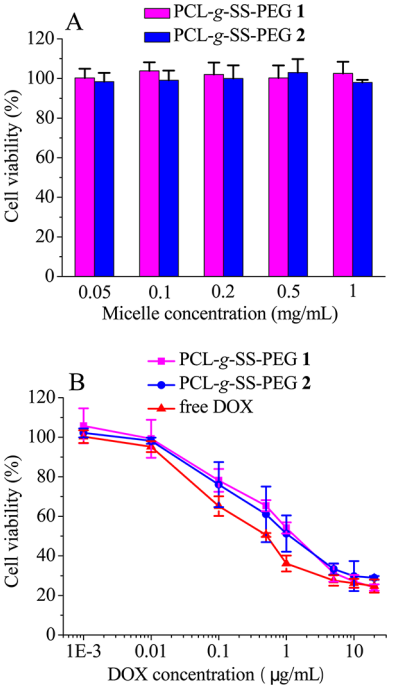

Figure 8. (A) Cytotoxicity of PCL-*g*-SS-PEG micelles to HeLa cells following 48 h incubation. (B) Viabilities of HeLa cells following 48 h incubation with DOX-loaded PCL-*g*-SS-PEG micelles and free DOX as a function of DOX dosages. All the data are presented as the average ± standard deviation (n = 4).

CONCLUSIONS

We have demonstrated that pyridyl disulfide-functionalized poly(ϵ-caprolactone) can be conveniently prepared with

dx.doi.org/10.1021/ma302499a | *Macromolecules* 2013, 46, 699−707

controlled molecular weights and functionalities by ring-opening copolymerization of ε-caprolactone with pyridyl disulfide cyclic carbonate monomer. To our knowledge, this represents a first report on synthesis of biodegradable polymers containing pendant multiple pyridyl disulfide groups. These pyridyl disulfide-functionalized biodegradable polymers provide a direct access to novel reduction-sensitive amphiphilic biodegradable graft copolymers that readily form micelles in water. Interestingly, these graft copolymer micelles exhibit excellent biocompatibility, enhanced stability with a low critical micelle concentration, and redox-triggered drug release behaviors. DOX-loaded micelles have shown pronounced antitumor activity to HeLa cells. This study has made a proof of concept that pyridyl disulfide-functionalized biodegradable polymers can be prepared and used for the construction of redox-responsive amphiphilic biodegradable graft copolymers and micelles that mediate efficient intracellular delivery of anticancer drugs.

AUTHOR INFORMATION

Corresponding Author

*Tel +86-512-65880098; e-mail zyzhong@suda.edu.cn.

Notes

The authors declare no competing financial interest.

ACKNOWLEDGMENTS

This work was supported by the National Natural Science Foundation of China (NSFC 51003070, 51103093, 51173126, and 51273139), the National Science Fund for Distinguished Young Scholars (51225302), Science and Technology Innovation Training Program (STITP 201210285020), and a Project Funded by the Priority Academic Program Development of Jiangsu Higher Education Institutions.

REFERENCES

(1) Nair, L. S.; Laurencin, C. T. *Prog. Polym. Sci.* **2007**, *32*, 762−798.
(2) Jerome, C.; Lecomte, P. *Adv. Drug Delivery Rev.* **2008**, *60*, 1056−1076.
(3) Tian, H.; Tang, Z.; Zhuang, X.; Chen, X.; Jing, X. *Prog. Polym. Sci.* **2012**, *37*, 237−280.
(4) Middleton, J. C.; Tipton, A. J. *Biomaterials* **2000**, *21*, 2335−2346.
(5) Ye, M.; Kim, S.; Park, K. *J. Controlled Release* **2010**, *146*, 241−260.
(6) Kim, H. K.; Chung, H. J.; Park, T. G. *J. Controlled Release* **2006**, *112*, 167−174.
(7) Melchels, F. P. W.; Feijen, J.; Grijpma, D. W. *Biomaterials* **2009**, *30*, 3801−3809.
(8) Lutolf, M. P.; Gilbert, P. M.; Blau, H. M. *Nature* **2009**, *462*, 433−441.
(9) Acharya, G.; Park, K. *Adv. Drug Delivery Rev.* **2006**, *58*, 387−401.
(10) Vasir, J. K.; Labhasetwar, V. *Adv. Drug Delivery Rev.* **2007**, *59*, 718−728.
(11) Deng, C.; Jiang, Y.; Cheng, R.; Meng, F.; Zhong, Z. *Nano Today* **2012**, *7*, 467−480.
(12) Zhang, X.; Mei, H.; Hu, C.; Zhong, Z.; Zhuo, R. *Macromolecules* **2009**, *42*, 1010−1016.
(13) Leemhuis, M.; van Nostrum, C. F.; Kruijtzer, J. A. W.; Zhong, Z. Y.; ten Breteler, M. R.; Dijkstra, P. J.; Feijen, J.; Hennink, W. E. *Macromolecules* **2006**, *39*, 3500−3508.
(14) Noga, D. E.; Petrie, T. A.; Kumar, A.; Weck, M.; Garcia, A. J.; Collard, D. M. *Biomacromolecules* **2008**, *9*, 2056−2062.
(15) Seow, W. Y.; Yang, Y. Y. *J. Controlled Release* **2009**, *139*, 40−47.
(16) Zhou, Y.; Zhuo, R. X.; Liu, Z. L. *Macromol. Rapid Commun.* **2005**, *26*, 1309−1314.
(17) Gerhardt, W. W.; Noga, D. E.; Hardcastle, K. I.; Garcia, A. J.; Collard, D. M.; Weck, M. *Biomacromolecules* **2006**, *7*, 1735−1742.
(18) Hu, X.; Chen, X.; Liu, S.; Shi, Q.; Jing, X. *J. Polym. Sci., Polym. Chem.* **2008**, *46*, 1852−1861.
(19) Pratt, R. C.; Nederberg, F.; Waymouth, R. M.; Hedrick, J. L. *Chem. Commun.* **2008**, 114−116.
(20) Tempelaar, S.; Mespouille, L.; Dubois, P.; Dove, A. P. *Macromolecules* **2011**, *44*, 2084−2091.
(21) Riva, R.; Schmeits, S.; Jerome, C.; Jerome, R.; Lecomte, P. *Macromolecules* **2007**, *40*, 796−803.
(22) Lu, C.; Shi, Q.; Chen, X.; Lu, T.; Xie, Z.; Hu, X.; Ma, J.; Jing, X. *J. Polym. Sci., Polym. Chem.* **2007**, *45*, 3204−3217.
(23) Parrish, B.; Breitenkamp, R. B.; Emrick, T. *J. Am. Chem. Soc.* **2005**, *127*, 7404−7410.
(24) Zhang, X.; Zhong, Z.; Zhuo, R. *Macromolecules* **2011**, *44*, 1755−1759.
(25) Mecerreyes, D.; Lee, V.; Hawker, C. J.; Hedrick, J. L.; Wursch, A.; Volksen, W.; Magbitang, T.; Huang, E.; Miller, R. D. *Adv. Mater.* **2001**, *13*, 204−208.
(26) Vaida, C.; Takwa, M.; Martinelle, M.; Hult, K.; Keul, H.; Möller, M. *Macromol. Symp.* **2008**, *272*, 28−38.
(27) Chen, W.; Yang, H.; Wang, R.; Cheng, R.; Meng, F.; Wei, W.; Zhong, Z. *Macromolecules* **2010**, *43*, 201−207.
(28) Onbulak, S.; Tempelaar, S.; Pounder, R. J.; Gok, O.; Sanyal, R.; Dove, A. P.; Sanyal, A. *Macromolecules* **2012**, *45*, 1715−1722.
(29) Feng, J.; Zhuo, R. X.; Zhang, X. Z. *Prog. Polym. Sci.* **2011**, *37*, 211−236.
(30) Tempelaar, S.; Mespouille, L.; Coulembier, O.; Dubois, P.; Dove, A. P. *Chem. Soc. Rev.* **2013**, *42*, 1312−1336.
(31) Chen, W.; Meng, F. H.; Li, F.; Ji, S. J.; Zhong, Z. Y. *Biomacromolecules* **2009**, *10*, 1727−1735.
(32) Chen, W.; Meng, F.; Cheng, R.; Zhong, Z. *J. Controlled Release* **2009**, *142*, 40−46.
(33) Xiong, J.; Meng, F.; Wang, C.; Cheng, R.; Liu, Z.; Zhong, Z. *J. Mater. Chem.* **2011**, *21*, 5786−5794.
(34) Yang, R.; Meng, F.; Ma, S.; Huang, F.; Liu, H.; Zhong, Z. *Biomacromolecules* **2011**, *12*, 3047−3055.
(35) Wu, Y.; Chen, W.; Meng, F.; Wang, Z.; Cheng, R.; Deng, C.; Liu, H.; Zhong, Z. *J. Controlled Release* **2012**, *164*, 338−345.
(36) Yu, Y.; Deng, C.; Meng, F.; Shi, Q.; Feijen, J.; Zhong, Z. *J. Biomed. Mater. Res., Part A* **2011**, *99A*, 316−326.
(37) Wang, R.; Chen, W.; Meng, F.; Cheng, R.; Deng, C.; Feijen, J.; Zhong, Z. *Macromolecules* **2011**, *44*, 6009−6016.
(38) Cheng, R.; Feng, F.; Meng, F.; Deng, C.; Feijen, J.; Zhong, Z. *J. Controlled Release* **2011**, *152*, 2−12.
(39) Meng, F.; Cheng, R.; Deng, C.; Zhong, Z. *Mater. Today* **2012**, *15*, 436−442.
(40) Meng, F.; Hennink, W. E.; Zhong, Z. *Biomaterials* **2009**, *30*, 2180−2198.
(41) Bulmus, V.; Woodward, M.; Lin, L.; Murthy, N.; Stayton, P.; Hoffman, A. *J. Controlled Release* **2003**, *93*, 105−120.
(42) Ryu, J.-H.; Jiwpanich, S.; Chacko, R.; Bickerton, S.; Thayumanavan, S. *J. Am. Chem. Soc.* **2010**, *132*, 8246−8247.
(43) Ryu, J.-H.; Chacko, R. T.; Jiwpanich, S.; Bickerton, S.; Babu, R. P.; Thayumanavan, S. *J. Am. Chem. Soc.* **2010**, *132*, 17227−17235.
(44) Cheng, R.; Wang, X.; Chen, W.; Meng, F.; Deng, C.; Liu, H.; Zhong, Z. *J. Mater. Chem.* **2012**, *22*, 11730−11738.
(45) Li, T.; Lin, J.; Chen, T.; Zhang, S. *Polymer* **2006**, *47*, 4485−4489.
(46) Lo, C.-L.; Huang, C.-K.; Lin, K.-M.; Hsiue, G.-H. *Biomaterials* **2007**, *28*, 1225−1235.
(47) Yu, Y.; Zou, J.; Yu, L.; Jo, W.; Li, Y.; Law, W.-C.; Cheng, C. *Macromolecules* **2011**, *44*, 4793−4800.
(48) Sun, H.; Guo, B.; Cheng, R.; Meng, F.; Liu, H.; Zhong, Z. *Biomaterials* **2009**, *30*, 6358−6366.
(49) Sanders, D. P.; Fukushima, K.; Coady, D. J.; Nelson, A.; Fujiwara, M.; Yasumoto, M.; Hedrick, J. L. *J. Am. Chem. Soc.* **2010**, *132*, 14724−14726.

(50) Wong, L.; Boyer, C.; Jia, Z.; Zareie, H. M.; Davis, T. P.; Bulmus, V. *Biomacromolecules* **2008**, *9*, 1934−1944.
(51) Sun, H.; Guo, B.; Li, X.; Cheng, R.; Meng, F.; Liu, H.; Zhong, Z. *Biomacromolecules* **2010**, *11*, 848−854.
(52) Tang, L.-Y.; Wang, Y.-C.; Li, Y.; Du, J.-Z.; Wang, J. *Bioconjugate Chem.* **2009**, *20*, 1095−1099.
(53) Liu, J.; Pang, Y.; Huang, W.; Huang, X.; Meng, L.; Zhu, X.; Zhou, Y.; Yan, D. *Biomacromolecules* **2011**, *12*, 1567−1577.
(54) Ren, T.-B.; Feng, Y.; Zhang, Z.-H.; Li, L.; Li, Y.-Y. *Soft Matter* **2011**, *7*, 2329−2331.
(55) Yoo, H. S.; Park, T. G. *J. Controlled Release* **2004**, *96*, 273−283.
(56) Zhang, W.; Li, Y.; Liu, L.; Sun, Q.; Shuai, X.; Zhu, W.; Chen, Y. *Biomacromolecules* **2010**, *11*, 1331−1338.